The ester crystallized from ethanol (25 mL) as white plates (0.56 g, 15%): mp 160.5–164.5 °C (lit.[1] mp 162–163 °C); homogeneous on TLC (C_6H_6–EtOH, 9:1). NMR (Me_2SO-d_6) δ 1.82 (3 H, s, 5-CH_3), 2.2 (2 H, t, 2′-CH_2), 4.05 (1 H, t, 4′-CH), 4.15–4.55 (4 H, c, 3′-CH and -OH, 5′-CH_2), 4.80 (2 H, s, CH_2CO_2), 5.08 (2 H, s, benzyl CH_2), 6.3 (1 H, t, 1′-CH), 6.95 (4 H, s, Ar), 7.45 (6 H, s, Ar and 6-CH). Anal. ($C_{25}H_{26}N_2O_8$) C, H, N.

Enzyme Preparation and Assay. L1210 ascites cells were suspended at 7×10^7 cells/mL in 50 mM Tris-HCl (pH 7.8), containing 150 mM KCl, and sonicated for two bursts of 15 s each. The sonicate was spun at 100 000*g* for 30 min, and the supernatant was brought to 30% saturation with a saturated ammonium sulfate solution. The resulting precipitate was resuspended in 50 mM Tris-HCl (pH 7.8) and used directly. All procedures were carried out at 4 °C. The heat-inactivated sample was prepared by incubation at 100 °C for 5 min. The enzyme preparation routinely had a V_m of 90–100 nmol h^{-1} (mg of protein)$^{-1}$.

Assay Procedure. 1. Radiochemical Assay. The assay mixture consisted of 2 mM ATP, 1 mM $MgCl_2$, 5 or 25 μM [^{3}H]TdR (100 μCi/μmol), 10% Me_2SO, 45 mM Tris-HCl (pH 7.8). The time course of the reaction at 37 °C was followed. Samples were taken at different times, and the reaction was stopped by boiling for 5 min. Aliquots of the reaction supernatant were spotted onto polyethylenimine cellulose squares (cut from Polygram cel 300 PEI plates), which were then washed three times in 5 mM Tris-HCl (pH 7.8) and once in 95% EtOH before drying. [^{3}H]TMP was eluted from the squares with 1 mL of 1 N HCl and counted with an efficiency of 30%.

2. Nonradiochemical Assay. The assay mixture was the same as for the radiochemical assay except that 0 or 5 μM unlabeled TdR was used. After 10 min of incubation at 37 °C, the reaction was stopped by dilution 20-fold with ice-cold water. This mixture was then diluted 10-fold with CH_3CN and passed through silica Seppaks (Waters Associates Ltd.) previously washed with CH_3CN–H_2O (9:1). The reaction tubes were washed with CH_3CN–H_2O (19:1) and the washings applied to the Seppaks, which were then washed with more CH_3CN–H_2O (19:1). This procedure washed through 99.9% of the applied thymidine but none of the TMP. The nucleotides were eluted with 10 mL of H_2O directly into round-bottom flasks, freeze-dried, redissolved in 1 mL of 25 mM $NaHCO_3$, and digested with alkaline phosphatase (4 units/mL) overnight. The nucleoside mixture was acidified with glacial acetic acid to about pH 5.5 and subjected to HPLC analysis, using a 23-cm 5μ C18 Apex column fitted with 2μ in-line filter, with a mixture (1:9) of MeOH and 50 mM succinic acid made to pH 5.7 with ammonia as solvent running at 1 mL/min. The absorbance at 254 and 280 nm was monitored, and the traces were analyzed by using a Trilab (Trivector, Sandy, Beds). To test recovery and reproducibility, control tubes were spiked with 1 μM TMP and processed with the assay tubes. Recovery was 102 ± 4% (mean ± SE for 14 determinations).

Thymidine Estimation. The thymidine in the samples was separated and quantitated by HPLC, using a 20 × 0.46 cm Spherisorb 5μ hexyl column running isocratically in 10% MeOH, 90% 25 mM acetic acid adjusted to pH 5.0 with ammonia, and fitted with 254- and 280-nm detectors.

Acknowledgment. This investigation was supported by Medical Research Council/Cancer Research Campaign grants. One of us (L.C.D.) thanks the Medical Research Council for a Research Studentship. We are indebted to Frances Boxall and Raymond Vincent for expert technical assistance and to Michael Baker for the mass spectral measurements.

Registry No. 1, 36983-61-6; 2, 90414-50-9; 3, 90414-51-0; 4, 90414-52-1; 5, 90414-53-2; 6, 25152-20-9; 7, 38559-92-1; 8, 90414-54-3; 9, 3351-59-5; 10, 67856-23-9; 11, 90414-55-4; cyclohexylamine, 108-91-8; 3′-*o*-tritylthymidine, 73189-04-5; thymidine, 50-89-5; thymidine kinase, 9002-06-6.

Structure–Activity, Theoretical, and X-ray Studies on the Intramolecular Interactions in a Series of Novel Histamine H_2 Receptor Antagonists

William C. Lumma, Jr.,[†,§] John J. Baldwin,*[,†] John B. Bicking,[†,⊥] William A. Bolhofer,[†] Jacob M. Hoffman,[†] Brian T. Phillips,[†] Charles M. Robb,[†] Mary Lou Torchiana,[†] H. B. Schlegel,[‡,∥] G. M. Smith,[‡] J. M. Hirshfield,[‡] J. P. Snyder,[‡] and J. P. Springer[‡]

Merck Sharp & Dohme Research Laboratories, West Point, Pennsylvania 19486, and Rahway, New Jersey 07065.
Received August 19, 1983

The furan ring of the histamine H_2 receptor antagonist 3-amino-4-[[2-[[[5-[(dimethylamino)methyl]-2-furanyl]-methyl]thio]ethyl]amino]-1,2,5-thiadiazole 1-oxide (**1a**) was replaced by thiophene, pyridine, benzene, and pyrrole. The relative receptor affinities of these analogues were estimated by in vitro and in vivo techniques. A theoretical model for the stacking interaction, observed by single crystal X-ray analysis of **1a**, was developed, and the ability to enter into this type of interaction was estimated. The X-ray analysis of the pyridine analogue of **1a** revealed no intramolecular stacking interaction. The theoretical studies were evaluated in light of the observed receptor affinities, and the relevance of the solid-state geometry of **1a** to the receptor-bound geometry was assessed. It is suggested that the stacked geometry found in the X-ray structure of **1a** does not represent a conformation that is relevant to that bound at the histamine H_2 receptor.

In a recent publication,[1a] the X-ray structure (Figure 1) of a novel, potent, and selective histamine H_2 antagonist, 3-amino-4-[[2-[[[5-[(dimethylamino)methyl]-2-furanyl]-methyl]thio]ethyl]amino]-1,2,5-thiadiazole 1-oxide (**1a**), was described.[1a,b] This report delineates attempts to optimize potency via an understanding of the intramolecular interactions found in the diaminothiadiazole class of histamine H_2 antagonists.

In the solid state, cimetidine, a clinically useful histamine H_2 receptor antagonist, adopts an intramolecularly folded structure stabilized by a hydrogen bond.[2] From

[†] Merck Sharp & Dohme Research Laboratories, West Point, PA.
[‡] Merck Sharp & Dohme Research Laboratories, Rahway, NJ.
[§] Present address: Berlex Laboratories, Inc., Cedar Knolls, NJ.
[⊥] Deceased Dec 28, 1982.
[∥] Wayne State University, Detroit MI 48202.

(1) (a) Anderson, P. S.; Baldwin, J. J.; Bolhofer, W. A.; Britcher, S. F.; Clineschmidt, B. V.; Denny, G. H.; Habecker, C. N.; Hirshfield, J. M.; Hirschmann, R.; Hoffman, J. M.; Lumma, W. C., Jr.; Phillips, B. T.; Pietruszkiewicz, A. M.; Randall, W. C.; Streeter, K. B.; Torchiana, M. L. *J. Med. Chem.* **1982**, *25*, 207. (b) Algieri, A. A.; Luke, G. M.; Standridge, R. T.; Brown, M.; Partyka, R. A.; Crenshaw, R. R. *J. Med. Chem.* **1982**, *25*, 210. (c) This work was presented in part at the 183rd National Meeting of the American Chemical Society, Las Vegas, NV, Mar 28, 1982; American Chemical Society: Washington, DC 1982; Abstr MEDI 59.
(2) Hadicke, E.; Frickel, F.; Franke, A. *Chem. Ber.* **1978**, *111*, 3222.

0022-2623/84/1827-1047$01.50/0

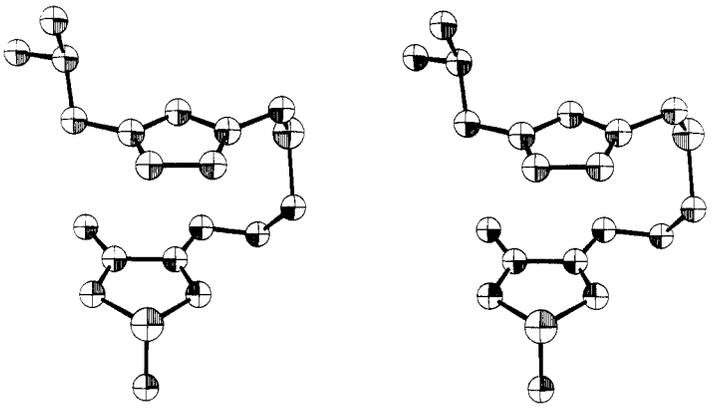

Figure 1. X-ray structure of **1a** viewed as a stereo pair.

Table I. MO Parameters for Parent Heterocycles; STO-3G Basis Set[a]

heterocycle	q_1	$q_{2,5}$	$q_{3,4}$	q	E_{HOMO}	E_{LUMO}
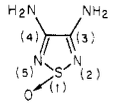	0.40[b]	−0.30[b]	0.23[b]	0.01[b] (NH_2)	−0.26[b]	0.21[b]
	−0.20	0.05	−0.10		−0.27	0.29
	0.25	−0.18	−0.08		−0.27	0.28
	−0.24	0.03 (2, 6)	−0.07 (3, 5)	−0.05 (4)	−0.30	0.24
	0.063	0.063	0.063	0.063	−0.28	0.27
	−0.31	0.02	−0.10		−0.24	0.33

[a] The geometries of the single rings were derived from STO-3G optimization. The thiadiazole ring was taken from single-crystal X-ray studies (ref 1). Comparison of the STO-3G optimized furan ring and that found by X-ray shows an average deviation of 0.017 Å for the heavy atom positions. The effects of movements of 0.02 Å in the electrostatic energy proportional to 1/dist will be far less than the differences computed for the various heterocycles (cf. Figure 3). [b] The STO-3G basis set was supplemented with d orbitals; STO-3G*.

a structure–activity study of cimetidine analogues, Mitchell[3] concluded that such a folded structure may be important for efficient oral absorption. In an attempt to determine factors that might stabilize the intramolecular stacking shown in Figure 1, we undertook a study of analogues of **1a**, in which benzene and various heterocycles replace the furan ring.

Theoretical Studies. For **1a**, as shown in Figure 1, the parallel planes of the diaminothiadiazole and furan rings are separated by 3.7–3.8 Å in the solid state. This geometric arrangement may be a result of electrostatic (ES) and charge-transfer (CT) interactions between the heterocyclic rings, as expressed by the GP equation (eq 1).[4]

$$E = \mathrm{ES} + \mathrm{CT} = \sum_{m,n} \frac{q_m^{\mathrm{D}} q_n^{\mathrm{A}}}{r_{\mathrm{DA}}\epsilon} + \sum_{m,n} \frac{(c_m c_n \Delta\beta_{m,n})^2}{E_{\mathrm{HOMO}} - E_{\mathrm{LUMO}}} \qquad (1)$$

Net atomic charges ($q_{m,n}$) and HOMO and LUMO energies were calculated at the STO-3G level of approximation[5] for the heterocyclic rings of **1a**, benzene and the parent heterocycles of **1b,c,e**, i.e., thiophene, pyridine, and pyrrole. The calculations are summarized in Table I. Geometries of the parent heterocycles were those of the minimum energy STO-3G structures,[5] except for that of 3,4-diamino-1,2,5-thiadiazole 1-oxide, which was taken from the X-ray coordinates of **1a**. These parameters were used in approximate assessments of the ES and CT interactions (eq 1) between the thiadiazole as an electron acceptor and the other ring systems as electron donors. In a related system involving hydroxyindoles and imidazolium ion, Weinstein et al.[6] were able to show that ES contributes about an order of magnitude more than CT to the binding energy, especially at separations approaching 4 Å.

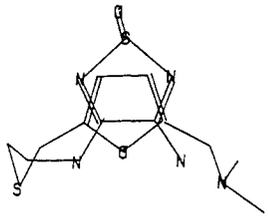

Figure 2. Vertical view of **1a** as seen in the X-ray.

A qualitative application of the data of Table I suggests that the optimal geometry for electrostatic attraction is the negatively charged furan oxygen above the positive C_3–C_4 thiadiazole region and the positively charged sulfur of the latter below the negatively charged furan C_3–C_4 region. This conformation is illustrated in Figure 2. These considerations also indicate that an almost identical arrangement might be possible for thiophene analogue **1b**. Since the dipole of the pyrrole is opposite to that of furan,[7] a favorable arrangement of pyrrole might be possible if its

(3) Mitchell, R. C. *J. Chem. Soc., Perkin Trans. 2* **1980**, 915.
(4) Klopman, G., Ed. "Chemical Reactivity and Reaction Paths"; Wiley: New York, 1974; p 60.
(5) Unpublished results of Dr. H. B. Schlegel; calculated with the program GAUSSIAN 78 (with gradient geometry optimization).
(6) Weinstein, H.; Osman, R.; Edwards, W. D.; Green, J. P. *Intl. J. Quantum Chem.: Quantum Biol. Symp.* **1978**, *No. 5*, 449–461. Osman, R.; Topiol, S.; Weinstein, H. *J. Comp. Chem.* **1981**, *2*, 73.
(7) Gialorenzo, M. *J. Heterocycl. Chem.* **1972**, *9*, 817. Barton, T. J.; Roth, R. W.; Verkade, J. W. *J. Am. Chem. Soc.* **1972**, *94*, 8854.

Scheme I

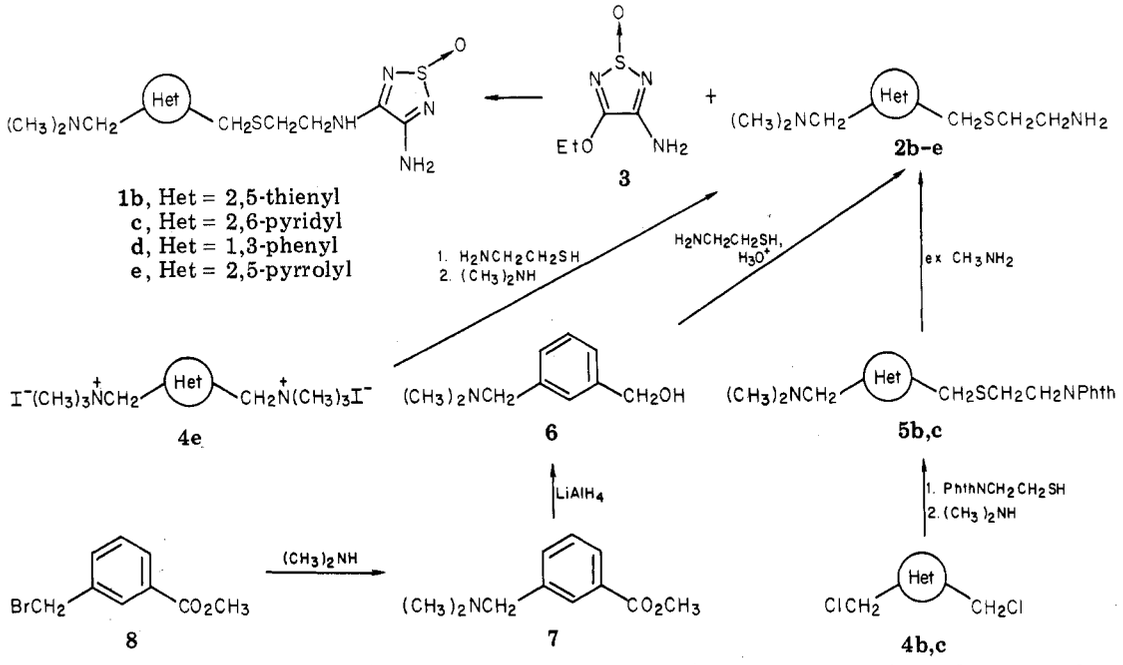

negative C_{2-5} region is oriented vertically above the thiadiazole $H_2N-C_{3,4}$ region and the nitrogen atom of the former occupies a region not projected on the thiadiazole ring.

To gain a more quantitative insight into the energy of electrostatic interactions, the ES term was calculated as a function of translation and rotation geometries by summing pairwise point-charge potentials with the aid of a computer program[8] and the Merck Molecular Modelling System.[9] An arbitrary interplanar distance of 3.85 Å, which approximates the X-ray results, was used. The geometries at all potential energy minima were visualized at this distance by computer graphics. The geometries for *selected* energy minima, including those most analogous to Figure 2, are shown in Figure 3, along with the deviations from overall minima (ΔE_{min}), for the various furan replacements.

The qualitative predictions, including the pyrrole case, are fully corroborated by the potential energy calculations. In every case, however, the overall minima correspond to a geometry in which the heterocycles are *not* superimposed. For furan, a minimum was found at geometry A, which resembles the stacking pattern in Figure 2. In the case of thiophene, the translated geometry B, shown in Figure 3, was not significantly different in energy from the nearly dipole opposed geometry C, which most closely resembles Figure 2. For pyrrole, no minimum was found at a geometry analogous to Figure 3A, but a superimposed geometry (Figure 3D) opposite to that of Figure 3A was not significantly different in energy from the overall minimum energy of the nonsuperimposed geometry (Figure 3E). Benzene was not included in this set of calculations because of the very small atomic charges arising from STO-3G (Table I). Furthermore, due to symmetry, the molecule presents no dipole in the plane of the ring.

Thiophene, pyrrole, and pyridine were then set at geometry A, and the potential energies were recalculated. The energies required to change the geometry from that at the global minimum (e.g., E for pyrrole) to geometry A for each of these heterocycles are also listed in Figure 3 ($E_A - E_{min}$). From these data it is clear that furan and pyridine are more stable than pyrrole and thiophene at geometry A by a factor of 5–10, though the energy differences are only 1–1.5 kcal.

The data of Table I suggest that the diaminothiadiazole 1-oxide is the best electron acceptor (E_{LUMO}). The STO-3G order of electron donor capacity (E_{HOMO}) is as follows: pyrrole > furan ≈ thiophene ~ benzene > pyridine. No quantitative estimate of the magnitude of the CT term in eq 1 was made, but its magnitude is expected to be about one-tenth that of ES because of poor orbital overlap at 3.85 Å.[6] Nevertheless, this term should increase as the $E_{HOMO} - E_{LUMO}$ term decreases. On this basis, the pyrrole, furan, and thiophene CT interactions should be slightly more stabilized than the benzene and pyridine interactions.

There are several simplifying assumptions inherent in the present computational work. The first is the usual one associated with drawing conclusions from gas-phase calculations as applied to molecules in the biophase. The situation is further complicated by the probability that the (dimethylamino)methyl side chain of furan is protonated in vivo and in vitro. We have not explicitly considered the protonated species. These simplifications are muted to a reasonable extent by the fact that only trends are being sought among a collection of very closely related structures. Differential solvation effects are thereby taken as constant. Neglect of the more serious influence of a charged side chain can, to a first approximation, likewise be regarded as a constant. In solution the charged center will be highly solvated and neutralized locally by its counterion. At the receptor, $[NH(CH_3)_2]^+$ is clearly associated with a charged protein moiety. In both instances, rotation about the CH_2 spacer between N^+ and the furan ring provides a mechanism for permitting intermolecular charge–charge interaction without involving the thiadiazole ring. For these reasons the calculated trends have been taken at face value for evaluation.

Chemistry. Analogues of **1a** were synthesized from amines **2** by reaction with 3-amino-4-ethoxy-1,2,5-thia-

(8) Program "SWEEP"; unpublished software composed by Dr. G. M. Smith of these laboratories. The program places pairs of heterocycles in parallel planes at a specified distance and calculates the summed pairwise net atomic charge potentials as a function of specified translation and rotation increments of one heterocycle relative to the other.

(9) Gund, P.; Andose, J. D.; Rhodes, J. B.; Smith, G. M. *Science* **1980**, *208*, 1425.

Table II. Physical Properties and Biological Data for Diaminothiadiazole 1-Oxides

no.	yield, %	mp, °C	rel[a] potency	−log K_B[b]	ED_{50}[c] mg/kg, iv	receptor affinity rank order
1a	*d*	145.5–146.5	0.18 (0.11, 0.30)	6.95	0.007 (0.003, 0.013)	+++
1b	40	143–147	NP[e]		0.008 (0.001, 0.070)	+++
1c	53	118.5–122.5	0.84 (0.57, 1.23)		0.170 (0.130, 0.220)	+
1d	20	126–130	0.51 (0.38, 0.69)		0.013 (0.006, 0.029)	++
1e	65	159–161	0.31 (0.23, 0.42)	6.85	0.170 (0.03, 0.94)	++

[a] All compounds tested at 0.1 μg/mL for their effect on the dimaprit-stimulated chronotropic response curve in the guinea pig right atrium in vitro; relative potency = ED_{30} without antagonist/ED_{30} with antagonist. [b] Intercept of the Schild plots when parallel dose–response curves were observed at more than one concentration. [c] Intravenous ED_{50} (95% confidence limits) for inhibition of histamine-stimulated gastric acid secretion in dogs (N = 4), in milligrams per kilogram. [d] Reference 1. [e] NP = not parallel.

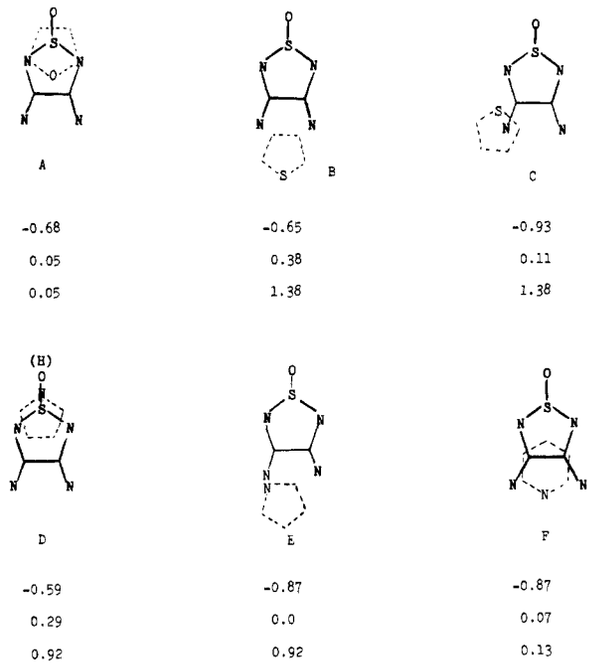

Figure 3. Selected electrostatic energy minima for heterocycles in parallel planes at a distance of 3.85 Å. Dotted structures are below the plane of the paper. The first numerical value accompanying each stacking complex is the point charge electrostatic stabilization energy relative to the separated rings. The second value is the energy difference of the pictured geometry from that of the global minimum (ΔE_{min}). The third value corresponds to the difference between the energies of each pair placed in the A geometry and that of the global minimum ($E_A - E_{min}$), in kilocalories per mole (cf. footnote *a* of Table I).

diazole 1-oxide (**3**),[10] as shown in Scheme I. The requisite amines **2b,c,e** were prepared by the sequential reaction of appropriately substituted heterocycles **4b,c,e** with cysteamine or its phthalimide derivative and dimethylamine. Intermediate **4e** was synthesized by quaternization of 2,5-bis[(dimethylamino)methyl]pyrrole[11] with 2 equiv of methyl iodide. Reaction of **4e** with cysteamine and aqueous base, followed by dimethylamine, gave 24% of amine **2e** and the bis displacement product as the major product. In the case of **2b,c**, the bis(chloromethyl)-substituted intermediates **4b,c** were sequentially reacted with *N*-(2-mercaptoethyl)phthalimide in the presence of tetramethylpiperidine and then with dimethylamine to give protected amines **5b,c**, which were deprotected with excess methylamine. The phenyl analogue **2d** was synthesized from methyl 3-(bromomethyl)benzoate (**8**). Reaction of **8** with dimethylamine gave amino ester **7**. The latter was reduced to alcohol **6** (LAH), which was reacted with cysteamine in aqueous HCl to give **2d**. Chemical and physical data for analogues **1a–e** are listed in Table II.

The crystal structure of **1c** was determined by an X-ray diffraction experiment on a sample grown from acetonitrile. Preliminary experiments showed that the symmetry was triclinic (subsequently found to be $P\bar{1}$) with cell parameters of a = 9.543 (7) Å, b = 9.903 (3) Å, c = 9.476 (8) Å, α = 108.35 (5)°, β = 96.96 (6)°, and γ = 81.24 (5)° for Z = 2. Of the 2259 unique data collected using an automatic four-circle diffractometer equipped with Cu $K\alpha$ radiation, 1810 were observed ($I \geq 3\sigma I$) and corrected for Lorentz and polarization effects.

The structure was solved by the multisolution tangent formula program MULTAN,[12] which provided two 20-atom fragments. Difference electron density syntheses provided the positions of the remainder of the atoms and indicated a second disordered position for the sulfur in each sulfide linkage. Hydrogen atoms were added, and positions, but not temperature factors, were refined. Full-matrix least-squares techniques were used to minimize the function $\sum\omega(|F_o| - |F_c|)^2$ with $\omega = 1/(\sigma F_o)^2$. The final unweighted residual was 0.064. Population parameters determined for S11, S11A, S11′, and S11A′ were 0.75, 0.25, 0.60, and 0.40, respectively. The two independent molecules have virtually identical enantiomeric conformations. However, the positions for the oxygens of the thiadiazole oxides clearly destroy this symmetry. The approximate symmetry and the disordered sulfides serve to introduce larger than normal errors in the refined structural parameters.

Each molecule has two intramolecular hydrogen bonds: N8–H8–N14, 2.98 Å; N7-H7B-N20, 2.89 Å; N8′-H8′-N14′, 2.80 Å; and N7′-H7′B-N20′, 2.82 Å. Two intermolecular hydrogen bonds connect the two molecules: N7-H7A-N2′, 2.89 Å, N7′-H7A′-N2, 2.96 Å. A computer-generated stereo ORTEP[13] drawing of structure **1c** is shown in Figure 4 with the two disordered positions of the sulfide indicated. Tables of the final coordinates, temperature parameters, bond lengths, and bond angles are available as supplementary material.

Discussion

Histamine H_2 receptor affinity was assessed in vitro by antagonism of the dimaprit-stimulated chronotropic response in guinea pig right atrial strips.[14] Nonparallel dose–response curves were observed at high antagonist

(10) Karady, S.; Amato, J. S.; Dortmund, D.; Reamer, R. A.; Weinstock, L. M. *Heterocycles* **1981**, *16*, 1561.
(11) Bachman, G. B.; Heisey, L. V. *J. Am. Chem. Soc.* **1946**, *68*, 2496.
(12) Main, P.; Woolfson, M. M.; Lessinger, L.; Germain, G.; Declerq, J. P. MULTAN 80 version. "A System of Computer Programs for the Automatic Solution of Crystal Structures from X-ray Diffraction Data", Universities of York, England, and Louvain, Belgium, 1978.
(13) Johnson, C. K. "ORTEP", report ORNL-3794; Oak Ridge National Laboratory: Oak Ridge, TN, 1965.
(14) Parsons, M. E.; Owen, D. A. A.; Gannelin, C. R.; Durant, G. J. *Agents Actions* **1977**, *7*, 31.

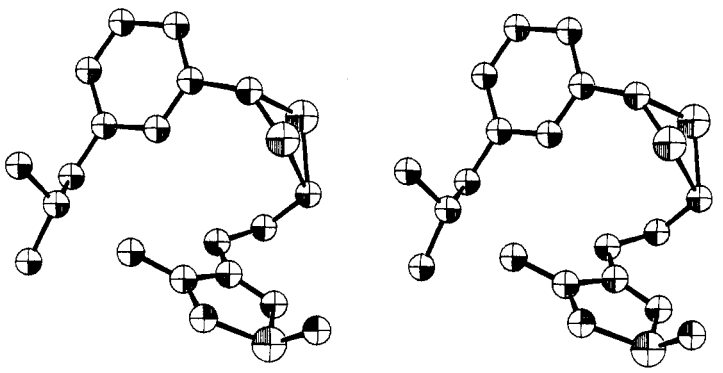

Figure 4. A computer-generated ORTEP stereo pair of the X-ray structure **1c**. Hydrogen atoms have been omitted for clarity.

concentrations, presumably because of slowly reversible binding of this class of compounds to the histamine H_2 receptor. Since the kinetics did not permit an estimation of pA_2 values, EC_{30} ratios for parallel curves with dimaprit as agonist in the absence and presence of antagonist (0.1 μg/mL) were thus used as a measure of receptor affinity. This treatment may impose limitations, and one should be cautious of an overinterpretation of the data. According to this relative potency data (Table II), analogues **1a,d,e** had greater receptor affinity than the pyridine analogue **1c**.

Blockade of histamine-stimulated gastric acid output in gastric fistula dogs[15] was also measured. The in vivo activity data supports this relative potency (except for **1e**) and places the thiophene analogue **1b** in the higher affinity group, assuming that antisecretory activity is a measure of histamine H_2 receptor affinity.

This rank order of activity is not in agreement with the calculated relative stability of the various heterocycles complexed with the diaminothiadiazole (vide supra); i.e., the derived stacking order clearly does not correlate with H_2 receptor affinities. The theoretical studies predict that the furan and pyridine analogues should have higher receptor affinities than the pyrrole and thiophene analogues if intramolecular interactions between heterocycles (vis., **1a**) are important in receptor binding.

An X-ray structure of the pyridine analogue (**1c**; Figure 4) revealed that in the solid state, intramolecular interaction did not involve parallel stacking of the heterocycles as for **1a** but, instead, involved hydrogen bonds between the pyridine nitrogen and the dimethylamino moiety with the weakly acidic hydrogens of the diaminothiadiazole end. This additional hydrogen bonding in **1c** stabilized a conformation different from the stacked conformation observed with **1a**. Thus, the relative stacking affinities of the heterocycles and the diaminothiadiazole in examples having $E_A - E_{min}$ values greater than for **1a** are not predictive of the solid-state geometry.

We conclude that the data of this study suggest that the geometry of Figure 1 does not represent the structure of **1a** as bound to the histamine H_2 receptor.

Experimental Section

All melting points were obtained on a Thomas-Hoover Unimelt capillary melting point apparatus on open capillaries and are uncorrected. Microanalytical results on all new compounds are indicated by atom symbols and are within ±0.4% of the theoretical values. NMR spectra were recorded on Varian T-60 and EM-390 spectrometers in $CDCl_3$–Me_4Si unless otherwise specified. Yields were not optimized and refer to the amount of analytical sample.

3-Amino-4-[[2-[[[5-[(dimethylamino)methyl]-2-pyrrolyl]methyl]thio]ethyl]amino]-1,2,5-thiadiazole 1-Oxide (1e). 2-[[[5-[(Dimethylamino)methyl]-2-pyrrolyl]methyl]thio]ethylamine (1.10 g, 5.5 mmol) was treated with a solution of 3-amino-4-ethoxy-1,2,5-thiadiazole 1-oxide (880 mg, 5.5 mmol) in 50 mL of CH_3CN. The mixture was stirred overnight at room temperature and filtered to give analytically pure **1e**: yield 1.1 g (65%); mp 159–161 °C dec; NMR (Me_2SO-d_6) δ 2.09 (s, 6 H), 2.5 (m, 1 H), 2.64 (t, 2 H), 3.27 (s, 2 H), 3.34 (broad s, 2 H), 3.49 (very broad s, 2 H), 3.71 (s, 2 H), 5.5 (dd, J = 1 Hz, 2 H), 7.60 (exchangeable, 1 H), 8.25 [exchangeable (sharp), 1 H], 8.30 (exchangeable, 1 H); mass spectrum (chemical ionization, negative ion), m/e 328. Anal. ($C_{12}H_{20}N_6OS_2$) C, H, N.

Compounds **1b–d** were prepared similarly, and results are summarized in Table II.

2-[[[5-[(Dimethylamino)methyl]-2-pyrrolyl]methyl]thio]ethylamine (2e). The 2,5-Bis[(trimethylammonio)methyl]pyrrole diiodide (23.5 g, 0.05 mol) was added to a stirred suspension of cysteamine hydrochloride (11.4 g, 0.01 mol) in 100 mL of CH_2Cl_2 at room temperature under N_2. The mixture was treated with benzyltributylammonium chloride (0.50 g) and 100 mL of 2 N NaOH (aq) and stirred at room temperature. The layers were separated, and the CH_2Cl_2 layer was dried over Na_2SO_4, filtered, and concentrated under vacuum to give 10.9 g of crude product, which was dissolved in 100 mL of absolute EtOH. The solution was treated with a solution of oxalic acid (2.70 g, 0.03 mol) in 100 mL of absolute EtOH. The resulting precipitate was collected by suction and dried under vacuum to give 10.5 g of crude 2,5-bis[[(2-aminoethyl)thio]methyl]pyrrole hydrogen oxalate, mp 190–191 °C dec.

The ethanol filtrate was concentrated under vacuum, and the residue was chromatographed on activity III alumina. Elution with $CHCl_3$–CH_3OH (0–5%) gave fractions containing 2.55 g (24%) of 2-[[[5-[(dimethylamino)methyl]-2-pyrrolyl]methyl]thio]ethylamine as a light yellow oil: NMR δ 2.13 (s, 6 H), 2.42 (A_2B_2, 4 H), 3.28 (s, 2 H), 3.63 (s, 2 H), 5.77 (broad s, 2 H), 1.97 (exchangeable, 2 H), 3.65 (exchangeable, 1 H). A sample of the amine was converted to an oxalate salt, mp 136–138 °C, in absolute ethanol. Anal. ($C_{10}H_{19}N_3S$·1.75($CO_2H)_2$·0.5H_2O) C, H, N.

2,5-Bis[(trimethylammonio)methyl]pyrrole Diiodide (4e). To a stirred solution of 2,5-bis[(dimethylamino)methyl]pyrrole[15] (9.0 g, 0.050 mol) in 200 mL of dry THF was added 6.0 mL (14.2 g, 0.10 mol) of CH_3I. The mixture was stirred for 4 h at room temperature and filtered to give the bis quaternary salt (23.5 g), mp 141–143 °C, which was not further purified.

2-[[[2-[(Dimethylamino)methyl]-5-thienyl]methyl]thio]ethylamine (2b). To a solution of 2,5-bis(chloromethyl)thiophene[16] (6.15 g, 34 mmol) in 35 mL of $CHCl_3$ and tetramethylpiperidine (5.9 mL, 34 mmol) at 70 °C was added dropwise a solution of *N*-(2-mercaptoethyl)phthalimide[17] (7.0 g, 34 mmol) in 35 mL of $CHCl_3$ during 1 h. After 4 h, the reaction mixture was cooled to room temperature, and dimethylamine gas was bubbled through the solution for 0.5 h. The chloroform solution was washed with H_2O and saturated Na_2CO_3 solution, dried over anhydrous Na_2SO_4, and then filtered, the filtrate was evaporated

(15) Bolhofer, W. A.; Hoffman, J. M.; Habecker, C. N.; Pietruszkiewicz, A. M.; Cragoe, E. J., Jr.; Torchiana, M. L. *J. Med. Chem.* **1979**, *22*, 301.

(16) Griffing, J. M.; Salisbury, L. F. *J. Am. Chem. Soc.* **1948**, *70*, 3416.

(17) Baddiley, J.; Thain, E. M. *J. Chem. Soc.* **1951**, 2253.

to give 15.7 g of crude product. The residue was dissolved in 70 mL of absolute EtOH, and the solution was saturated with methylamine gas. The solution was stirred for 2–3 days as *N,N'*-dimethyl-2-phthalic dicarboxamide slowly precipitated. The mixture was diluted with 70 mL of diethyl ether, and the precipitated byproduct was filtered off. The filtrate was evaporated to give 6.4 g, which was further purified by distillation to give 2.4 g of **2b**: bp 131–136 °C (0.3 mm) (31% overall yield): NMR δ 2.25 [s, 6 H, $(CH_3)_2N$], 2.70 (m, 4 H, CH_2CH_2), 3.54 (s, 2 H, CH_2), 3.84 (s, 2 H, CH_2), 6.68 (quat, 2 H, J_{AB} ~1.5 Hz, furan).

2-[[[6-[(Dimethylamino)methyl]-2-pyridyl]methyl]thio]-ethylamine (2c). Into the solution of 6-[(dimethylamino)-methyl]-2-[[(2-phthalimidoethyl)thio]methyl]pyridine (48.92 g, 0.137 mol) in MeOH (350 mL) was bubbled methylamine until 42.5 g (1.37 mol) had been added. The resulting warm solution was cooled to room temperature and stirred for 2.5 days in a sealed flask. The solution was concentrated in vacuo to one-third volume, and the resulting precipitate was filtered off. The filtrate was concentrated to dryness, and the residue was triturated with ether. The ether solution was concentrated to dryness to give a viscous yellow oil (14.94 g). The solid (28.0 g) was extracted with MeOH (50 mL). The methanol solution was concentrated to dryness, the residue was triturated with ether, and filtered, and the ether solution was concentrated to give an additional 2.45 g of yellow oil. The combined oil was distilled to give the product (9.63 g, 30%): bp 138–143 °C (0.3 mm); NMR δ 1.3 (broad s, 2 H, exchangeable), 2.2 (s, 6 H), 2.5–2.9 (m, 4 H), 3.5 (s, 2 H), 3.8 (s, 2 H), 7.1–7.7 (m, 3 H).

6-[(Dimethylamino)methyl]-2-[[(2-phthalimidoethyl)-thio]methyl]pyridine (5c). To the solution of *N*-(2-mercaptoethyl)phthalimide[17] (25.91 g, 0.125 mol) in MeOH (200 mL) was added NaOMe (6.75 g, 0.125 mol). The mixture was warmed until a clear yellow solution formed, and this was added to a solution of 2,6-bis(chloromethyl)pyridine[18] (22.00 g, 0.125 mol) in MeOH (350 mL) cooled to 5 °C (ice bath). After an exotherm (temperature rose to 15 °C), the solution was stirred while warming to room temperature over a 3-h period. The mixture was filtered and cooled to 10 °C, and a solution of dimethylamine (11.27 g, 0.250 mol) in MeOH (50 mL) was added. The mixture was stirred with gradual warming to room temperature over 16 h and then filtered, and the filtrate was concentrated in vacuo to give 64.08 g of a yellow gum. The gum was taken up in 350 mL of water, cooled to 5 °C, and acidified with 6 N HCl solution. The resulting solution was filtered, and the filtrate was made basic with saturated $NaHCO_3$ solution and extracted with $CHCl_3$. The organic layers were combined, dried over Na_2SO_4, and filtered, and the filtrate was concentrated in vacuo to give the product (24.5 g, 55%) as a viscous yellow oil, which was not further purified: NMR δ 2.2 (s, 6 H), 2.8 (s, 2 H), 3.1 (s, 2 H), 3.5 (s, 2 H), 3.9 (s, 2 H), 7.1–7.8 (m, 7 H).

2-[[3-[(Dimethylamino)methyl]benzyl]thio]ethylamine (2d). Cysteamine hydrochloride (7.56 g, 0.067 mol) was dissolved in 25 mL of 48% aqueous HBr under N_2, and the solution was treated with 3-[(dimethylamino)methyl]benzyl alcohol (10.0 g, 0.061 mol). The mixture was heated for 24 h over steam and under N_2; after cooling in an ice bath, the solution was basified with 10 N NaOH. The liberated amine was extracted with CH_2Cl_2. The CH_2Cl_2 extracts were combined, dried (Na_2SO_4), and filtered, and the filtrate was concentrated under vacuum to give 13.4 g of crude 2-[[3-[(dimethylamino)methyl]benzyl]thio]ethylamine. A sample was converted to the hydrochloride salt, mp 176–177 °C (lit.[19] mp 180–182 °C) in methanol/2-propanol.

3-[(Dimethylamino)methyl]benzyl Alcohol (6). To a stirred suspension of $LiAlH_4$ (8.89 g, 0.234 mol) in 250 mL of ether under N_2 was added dropwise a solution of methyl 3-[(dimethylamino)methyl]benzoate (56.6 g, 0.293 mol) in 115 mL of ether. The mixture refluxed spontaneously during the addition, and reflux was continued for an additional 1 h. After cooling in an ice bath, the mixture was treated dropwise with a solution of 8.9 mL of 15% aqueous NaOH in 33.5 mL of water. The resulting suspension was filtered, and the filtrate was dried ($MgSO_4$), filtered, and concentrated under vacuum to give 46.3 g (96%) of the product amino alcohol. Distillation gave a fraction with bp 100–103 °C (0.2 mm): yield 25 g (52%); NMR δ 7.27 (m, 4 H), 4.58 (s, 2 H), 3.37 (s, 2 H), 2.15 (s, 6 H).

Methyl 3-[(Dimethylamino)methyl]benzoate (7). To a solution of dimethylamine (71.68 g, 1.59 mol) in 200 mL of ether at 5 °C was added methyl 3-(bromomethyl)benzoate[20] (145.7 g, 0.636 mol) during 45 min. The resulting mixture was stirred while warming to room temperature as the ice bath melted and then overnight at room temperature. The mixture was filtered, and the filtrate was concentrated under vacuum to give 134 g of an oil. Distillation gave a fraction, bp 95–97 °C (0.2 mm), of colorless amino ester, yield 56.6 g (46%); NMR δ 7.83 (m, 2 H), 7.33 (m, 2 H), 3.87 (s, 3 H), 3.43 (s, 2 H), 2.23 (s, 6 H).

Acknowledgment. The authors are indebted to J. P. Moreau for chemical analyses, to P. G. Cook, C. A. Hanson, C. A. Wesley, S. R. Weise, and J. M. Stavorski for expert technical assistance, and to M. Z. Banker for manuscript preparation.

Registry No. **1b**, 78467-83-1; **1c**, 87107-88-8; **1d**, 78441-87-9; **1e**, 89999-71-3; **2b**, 69340-31-4; **2c**, 78442-44-1; **2d**, 69384-24-3; **2d**·HCl, 89999-75-7; **2e**, 89999-72-4; **2e**·oxalate, 89999-73-5; **3**, 79844-91-0; **4c**, 3099-28-3; **4e**, 89999-74-6; **5c**, 83592-47-6; **6**, 69383-72-8; **7**, 89999-70-2; **8**, 1129-28-8; cysteamine hydrochloride, 156-57-0; 2,5-bis[[(2-aminoethyl)thio]methyl]pyrrole, 90028-86-7; 2,5-bis[[(2-aminoethyl)thio]methyl]pyrrole oxalate, 90028-87-8; 2,5-bis[(dimethylamino)methyl]pyrrole, 89999-76-8; 2,5-bis-(chloromethyl)thiophene, 28569-48-4; *N*-(2-mercaptoethyl)-phthalimide, 4490-75-9.

Supplementary Material Available: Tables I–III containing fractional unit cell coordinates, bond lengths, and bond angles and a figure showing the arbitrary crystallographic numbering system for structure **1c** and hydrogen bond parameters as determined by X-ray diffraction (6 pages). Ordering information is given on any current masthead page.

(18) Baker, W.; Buggle, K. M.; McOmie, J. F. W.; Watkins, D. A. M. *J. Chem. Soc.* **1958**, 3594.

(19) Belgian Patent 867 106, 1978.

(20) Fuson, R. C.; Cooke, H. G., Jr. *J. Am. Chem. Soc.* **1940**, *62*, 1180.